Available online at www.sciencedirect.com

SciVerse ScienceDirect

Ceramics International 39 (2013) 7605–7611

CERAMICS INTERNATIONAL

www.elsevier.com/locate/ceramint

Synthesis of high magnetization hydrophilic magnetite (Fe_3O_4) nanoparticles in single reaction—Surfactantless polyol process

Mohamed Abbas[a,c], B. Parvatheeswara Rao[b], S.M. Naga[c], Migaku Takahashi[a,d], CheolGi Kim[a,*]

[a]*Center for NanoBioEngineering and Spintronics, Department of Materials Science and Engineering, Chungnam National University, Daejeon 305-764, Republic of Korea*

[b]*Department of Physics, Andhra University, Visakhapatnam 530003, India*

[c]*Ceramics Department, National Research Centre, 12311Cairo, Egypt*

[d]*New industry Creation Hatchery Center, Tohoku University, Aoba-yama 10, Sendai 980-8579, Japan*

Received 28 January 2013; received in revised form 19 February 2013; accepted 5 March 2013
Available online 14 March 2013

Abstract

High magnetization hydrophilic magnetite nanoparticles have been synthesized in two different batches with mean particle sizes of 32.3 and 9.2 nm by inexpensive and surfactant-free facile one-pot modified polyol method. In the synthesis, polyethylene glycol was used as a solvent media and it has been found to play a key role to act as a reducing agent as well as a stabilizer simultaneously. It was shown that the size of the nanoparticles can be effectively controlled by modifying the reaction parameters such as reaction temperature, time and polyol/metal precursor ratio. X-ray diffraction and energy dispersive spectroscopy studies confirm the formation of a pure magnetite phase without the presence of any other phases. Transmission electron microscopy and the Fourier transform infrared spectroscopy results reveal that the particle size and surface adsorption properties are very much dependent on reaction parameters. The magnetic properties of the samples measured by physical property measurement system have shown that the as-synthesized magnetite nanoparticles possess a high magnetization of 85.87 emu/g at 300 K and 91.7 emu/g at 5 K with negligible coercivities. The structural and magnetic characterizations of these polyol coated, hydrophilic, monodisperse, superparamagnetic nanoparticles clearly indicate that they are suitable for biomedical applications.

Keywords: High magnetization; Hydrophilic; Magnetite nanoparticles; Polyol process

1. Introduction

Magnetite (Fe_3O_4) nanoparticles with excellent structural and magnetic properties are considered to be highly promising magnetic materials for biomedical applications due to their non-toxicity and high chemical stability [1]. It means, magnetic nanoparticles to be used in bioapplication systems should possess some of the physical features like small size, uniform size distribution, superparamagnetic nature with high magnetic moment besides the solubility in water so as to make them suitable for applications such as targeted drug delivery, hyperthermia and magnetic resonance imaging enhancement [2]. In addition, magnetic nanoparticles are also used as magnetic labels for applications such as cell separation, manipulation and biomolecule detection in which the particle sizes can have the flexibility to be slightly larger to accommodate the presence of multiple ligands on the particle surface and to achieve multivalent interactions. In this latter case, the magnetic labels often come as nanoparticle encapsulated biocompatible polymer beads with the properties of large magnetization and good chemical stability [3]. These labels/beads, as a result of the coupling of the many adjacent encapsulated magnetic spins, tend to exhibit good magnetic performance so as to generate sufficient levels of stray fields for efficient detection on successful bio-interaction. Nevertheless, since the applicability of the magnetic nanoparticles in the biosystems demand high saturation magnetization and biocompatibility as

*Corresponding author. Tel.: +82 1044356632.
E-mail address: cgkim@cnu.ac.kr.(C. Kim)

0272-8842/$ - see front matter © 2013 Elsevier Ltd and Techna Group S.r.l. All rights reserved.
http://dx.doi.org/10.1016/j.ceramint.2013.03.015

basic requirements, the development of magnetite nanoparticles, which are known for their high biocompatibility and high magnetization, has therefore become an obvious choice for intense investigations.

Recently, with the advent of several wet chemical methods for the synthesis of nanoparticles, many groups have worked to synthesize magnetite nanoparticles using different methods such as solvothermal [4], sol–gel [5], coprecipitation [6], thermal decomposition [7], citrate gel [8], etc. Though all these methods provide great benefits in the control of size, component and dispersion, they however suffer from certain disadvantages too such as consumption of large amounts of surfactant, long synthesis times, etc. Moreover, some of these methods may even require deoxygenated protection and process in organic phase to yield hydrophobic nanoparticles which further need additional modifications to be hydrophilic for use in bio-applications. Besides, toxic gases like carbon monoxide might be emitting in the case of thermal decomposition method. However, the polyol method which involves reduction of metal salts with a diol, typically ethylene glycol, diethylene glycol, or a mixture of both is believed to be one of the most appropriate methods for synthesis of hydrophilic nanoparticles as it amply provides the possibility to control the experimental conditions kinetically and to scale up easily [9]. Also, by using the polyol process we can dispense the use of surfactant, because the polyethylene glycol (PEG) plays a triple role as high-boiling solvent, reducing agent, and stabilizer to efficiently control the particle growth and prevent inter-particle aggregation due to steric interactions, in addition to its hydrophilic properties [10]. Thus, there have been some efforts to this effect by some of the research groups and reported the results on the synthesis of magnetite nanoparticles using different kinds of polyol such as ethylene glycol, diethylene glycol, tri-ethylene glycol, tetra-ethylene glycol and propylene glycol [11–14]. In these works, apart from using different kinds of polyol, deoxygenated protection of the reaction and in some cases additives and long time reactions were also used to obtain monodisperse, water soluble magnetite nanoparticles with saturation magnetizations in the range from 45 to 77 emu/g.

Herein, we report a one-pot facile polyol method for the preparation of high magnetization hydrophilic Fe_3O_4 nanoparticles without using any surfactant and deoxygenated conditions, while realizing the possibility for controlling the size of the nanoparticles by varying some of the reaction parameters. The structure, composition, size, surface coating, thermal and magnetic properties of the synthesized nanoparticles were examined in detail and discussed the obtained results.

2. Materials and methods

2.1. Materials

High purity analytical reagent grade iron chloride tetrahydrate ($FeCl_2{\cdot}4H_2O$), polyethylene glycol (PEG), sodium hydroxide (NaOH) and ethyl alcohol were purchased from Sigma Aldrich and used in synthetic reaction without any further treatment.

2.2. Synthesis of magnetite nanoparticles

Synthesis of magnetite nanoparticles was made in two different batches to verify the influence of the reaction parameters on the particle size as well as their magnetic performance. In the first batch of reaction, hereafter typically referred as sample-I, we dissolve 24 mM of $FeCl_2{\cdot}4H_2O$ in 80 ml of PEG using magnetic stirrer in a 250 ml three-neck round bottomed flask equipped with condenser, magnetic stirrer, thermometer and heating system. The pH of the solutions was adjusted in between 10 and 11 by adding NaOH. The PEG–metal salts solution was then gradually heated up to 300 °C while stirring continuously using a magnetic stirrer, and refluxed at this temperature for 2 h. Then the solution was naturally cooled down to room temperature, washed several times using ethanol and water and collected the precipitate using a magnet. It was subsequently dried in a vacuum oven to obtain ultrafine magnetite nanoparticles.

In another reaction, herein after referred to as sample-II, the synthesis procedure follows the same steps as observed in the case of sample-I but with two modifications in reaction conditions, namely (i) the amount of precursor weight to be at 12 mM of $FeCl_2{\cdot}4H_2O$ in 80 ml of PEG, and (ii) keep the solutions at 200 °C for 30 min while heating before increasing the temperature to 300 °C for refluxing a period of 2 h. These modifications in the reaction parameters are expected to bring changes not only in the particle size and size-distribution but also in the magnetic behavior of the resultant magnetite nanoparticles.

2.3. Characterization

Structural characterizations were performed by X-ray diffraction (XRD) analysis using Rigaku RiNT 2200, which was carried out at the voltage of 40 kV and the current of 40 mA, by employing a scanning rate of 2 deg/min and a step size of 0.01 in the 2θ range from 20° to 80° with Cu K_α radiation. The size and morphology of the synthesized nanoparticles were characterized using Tecnai G2 F20 Scanning/Transmission electron microscope (S/TEM) with field emission system operated at 200 kV. The selected area electron diffraction (SAED) images were also recorded using the S/TEM. Energy dispersive spectroscopy (EDS), which was mounted on S/TEM, was used for elemental analysis. Fourier transform infrared (FTIR) spectroscopic data was taken in the range from 4000 to 400 cm^{-1} to interpret the traces of surface coating of PEG on the nanoparticles. Thermogravimetric analyses (TGA) were performed on the samples with a heating rate of 5 °C/min from room temperature up to 800 °C using a Material Analysis and Characterization TG-DTA system to observe the weight loss during heating. The magnetic properties of the synthesized nanoparticles were measured by physical property measurement system (PPMS) of Quantum Design Inc. with an external magnetic field ranging from −30 kOe to +30 kOe.

3. Results and discussion

3.1. Crystal structure and size

The X-ray diffraction patterns of the synthesized magnetite nanoparticles of both the batches, sample-I (a) and sample-II (b), are shown in Fig. 1. The peaks can be indexed at the values of 30.1°, 35.4°, 37.0°, 43.0°, 53.39°, 56.9°, 62.6°, 70.9°, 73.9° and 78.9° corresponding to the crystal planes of (220), (311), (222), (400), (422), (511), (440), (620), (533) and (444), respectively.

The strong peaks with minimal background noise clearly indicate the formation of fully crystalline iron oxide with a cubic inverse spinel structure, which are consistent with the standard data for magnetite (JCPDS Card no.00-019-0629). No peaks of any other phases are observed in the XRD patterns of the particles, thus indicating the high purity of the magnetite. Also, the black color of the product further testifies that it contains solely the magnetite phase and not that of the maghemite phase (brown color) as both these phases display the same spinel structure with similar XRD patterns [15].

Fig. 2 shows the typical EDS pattern of the as-synthesized (sample-I) magnetite nanoparticles. The pattern quantitatively describes the presence of Fe and O elements in the sample whereas the obtained Cu and C peaks are due to carbon copper grid employed in the measurements. The EDS analysis of the pattern facilitates estimation of oxygen and iron concentrations in the sample as 75.3% and 24.7%, respectively. While taking into account the atomic weights of iron and oxygen as 55.847 and 15.999, the weight percentage of iron and oxygen concentrations in the sample was estimated, and the ratio of elements comes close to the empirical formula of Fe_3O_4 and thus confirms that the obtained nanoparticles were that of the magnetite only.

The crystallite size of the sample-I was calculated from the XRD pattern using the Scherrer equation

$$D = K\lambda/\beta\cos\theta \quad (1)$$

where λ is the X-ray wavelength (1.540562 Å), β is the full width at half maximum (FWHM), θ is the Bragg angle for the studied peak/ring, and K is the shape factor which is normally taken as 0.9 for magnetite and maghemite [16]. We applied this equation to the best fitting highest intensity (311) XRD peak and estimated the crystallite size to be about 30 nm, which is in commensurate with the mean size of the nanoparticles (32.3 ±0.6 nm) obtained from the typical TEM image of the same sample (Fig. 3b). The slight difference in the particle size from the XRD and the TEM measurements can be explained as follows: since the crystallite size is inversely proportional to the FWHM, it implies that the crystallite size is larger for a smaller peak broadening and vice versa. Therefore, it is quite natural that the Scherrer formula provides relatively a smaller value for the particle size as the width of the diffraction peak is caused by, apart from the particle size, a variety of other factors including inhomogeneous strain and instrumental effects [17]. At the same time, it is possible that the nanoparticles synthesized by polyol method are likely to be surface coated by polyol ligands and the corresponding estimation of the mean particle size through lognormal distribution from the TEM images would also give relatively a larger estimate compared to the actual particle size and thus explains the observed difference. However, the crystallite size estimated by the Scherrer formula for Sample-II through the high intensity 311 peak broadening of the corresponding XRD pattern is found to be about 9 nm, and this is in close agreement with the estimated particle size of 9.2±0.3 nm from the TEM image (Fig. 3d) of the same sample. Therefore, it can be understood from the above that the relative contributions by the inhomogeneous strain and the instrumental effects to the XRD peak broadening are negligibly small, and also the thickness of PEG coating on the surface of the nanoparticles is very thin in the sense that their contributions lie within the experimental error in determining the particle sizes.

3.2. Morphology

The obtained magnetite nanoparticles were partly spherical and partly faceted in shape, as observed by S/TEM images shown in Fig. 3a–d. The SEM image of sample-I in Fig. 3a reveals that the particles are apparently uniform in size and

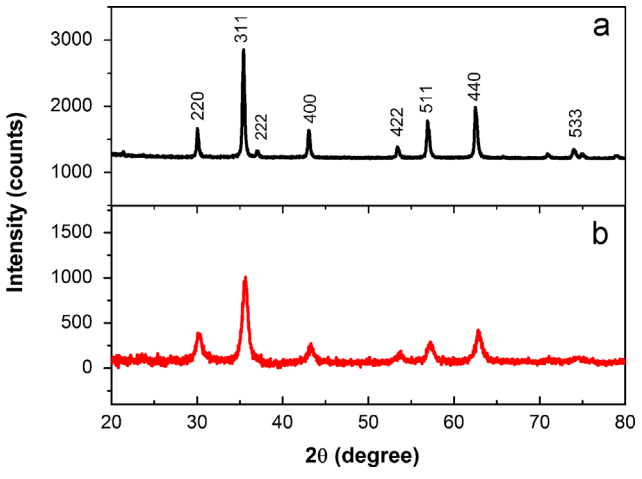

Fig. 1. XRD patterns of the synthesized magnetite nanoparticles; (a) Sample-I and (b) Sample-II.

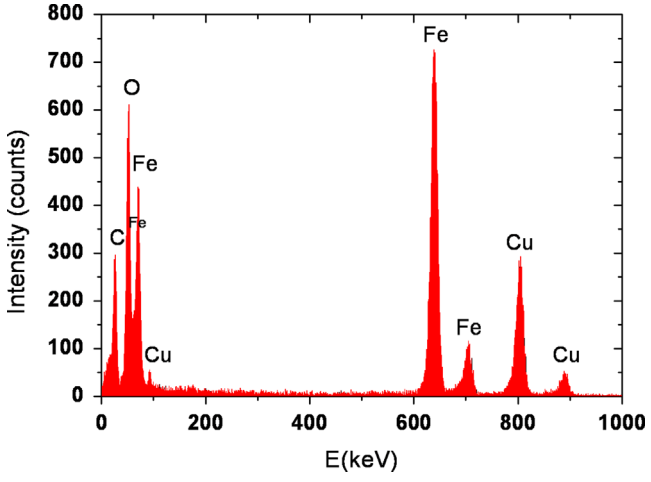

Fig. 2. Typical EDS pattern of the magnetite nanoparticles showing the presence of Fe and O elements in the nanoparticles (Cu and C peaks are due to carbon copper grid).

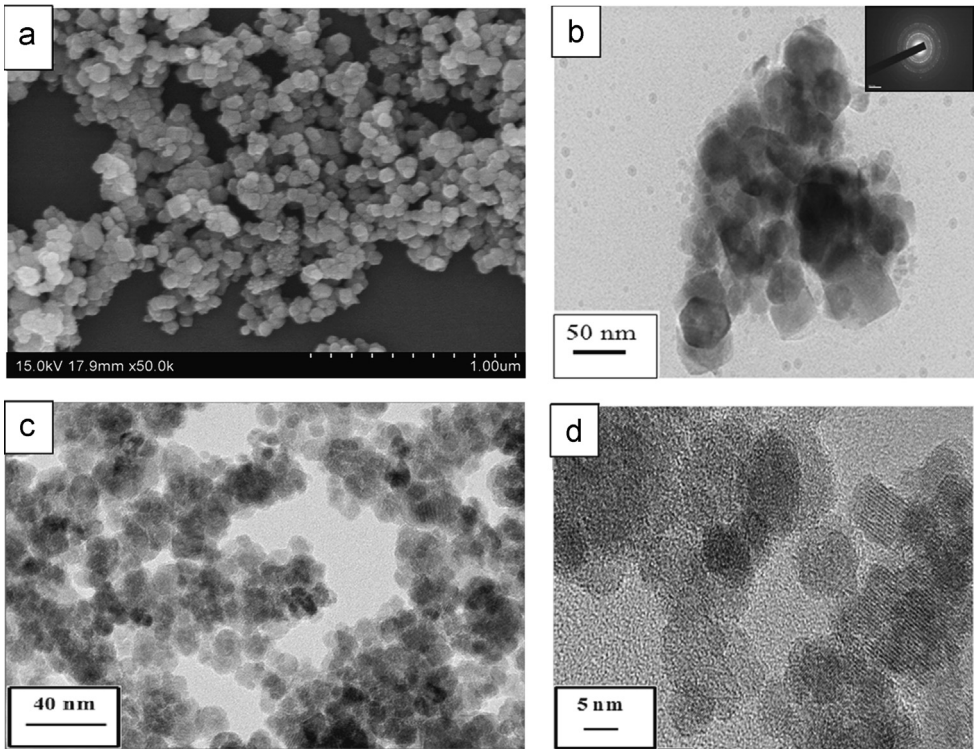

Fig. 3. (a) SEM image of Sample-I characterized by size distribution, (b) TEM image of Sample-I with mean particle size of about 32.3±0.6 nm; inset of the figure shows the selected area electron diffraction pattern of the sample, (c) TEM image of Sample-II characterized by size distribution, and (d) TEM image of Sample-II with mean particle size of about 9.2±0.3 nm.

the distribution is also appeared to be narrow. And, Fig. 3b shows the typical TEM image of the same sample, where the magnetite nanoparticles in a closer view reveal their spherical and faceted shapes more clearly with the average mean size of about 32.3 nm. As discussed earlier and also evident from the TEM image, this larger size of the nanoparticles, compared to the crystallite size obtained from the Scherrer method, has been attributed to the additional contribution of a thin layer of PEG which formed as a shell surrounding the core during the synthesis reaction of the magnetite nanoparticles. The inset of Fig. 3b, which shows the selected area electron diffraction pattern of sample-I, exhibits a good crystalline nature of the magnetite corresponding to a cubic structure in conformity with the XRD measurements.

The TEM images of sample-II, for which the reaction parameters are modified in terms of the ratio of iron precursor ($FeCl_2{\cdot}4H_2O$) to the solvent media (PEG) and the heating schedule, are shown in Fig. 3c,d. As expected, the modified reaction conditions resulted in size reduction of the particles to be about 9.2 nm as demonstrated in the figures. The decrease in the particle size may be attributed to increased amount of PEG with respect to the iron precursor, where it is well known that the PEG is characterized by its strongest reducing properties, which lead to the formation of a thin monolayer of the PEG on the surface of the nanoparticles not only to stabilize the particles in the solution but also to act as a protective agent to inhibit the particle growth. Also, the soaking time of 30 min at the temperature of 200 °C in the reaction could lead to a slow nucleation and growth for the magnetite particles in synthesis and thus contributes significantly for the small size of the particles in this sample. Moreover, the thin layer of PEG, due to its known biocompatibility and hydrophilic properties, present on the surface of the nanoparticles greatly improves the requirement of obtaining stable aqueous suspensions in water as well as in many organic solvents. This is amply demonstrated by dispersing the magnetite nanoparticles of sample-II with mean particle size of about 9.2 nm in ethanol and water, as shown in Fig. 4a and b, respectively. The sample showed very good dispersability in both the media and this is attributed to the formation of a steric barrier given from the strong hydrophilic PEG ligands coated on the nanoparticles during the synthesis process.

3.3. FTIR study

Further experimental evidence in support of the formation of a thin PEG layer on the particle surface is obtained through the FTIR spectrum, as shown in Fig. 5. The two broad bands observed between 3650 and 2950 cm^{-1} while centering at about 3380 cm^{-1} and 1650–1550 cm^{-1} with centered wave number at about 1608 cm^{-1} due to the O–H stretching vibrations, and the small peaks at about 1356 and 1074 cm^{-1} due to C–H bending and O–H bending, respectively are attributed to the adsorbed polyol molecules and thus confirmed the coating of thin PEG ligands onto the particle surface [12,18]. Besides, the spectrum clearly depict the major characteristic absorption bands of magnetite at about 542 and 400 cm^{-1} due to Fe_A–O and Fe_B–O stretching vibrations and these could be assigned to the

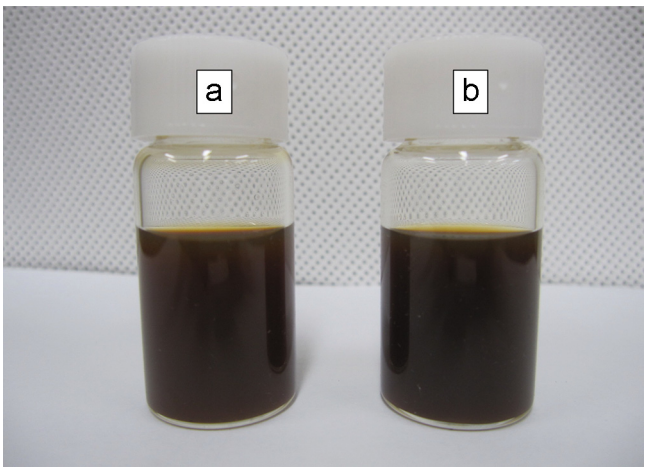

Fig. 4. Dispersibilty of the magnetite nanoparticles of Sample-II in (a) ethanol and (b) water.

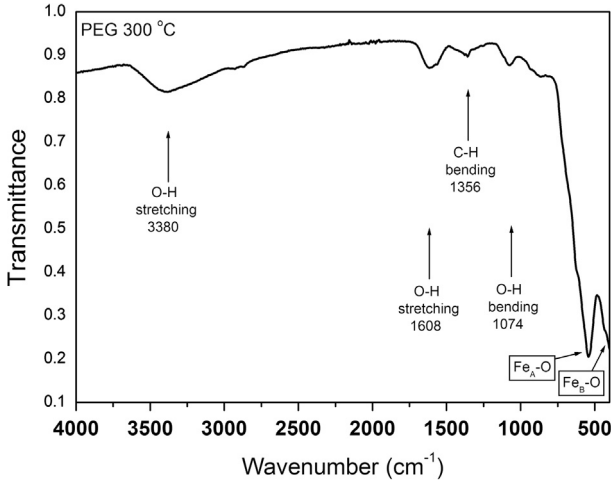

Fig. 5. FTIR spectrum showing the traces of coating of a thin layer of PEG on the surface of the magnetite nanoparticles of Sample-II.

tetrahedral and octahedral Fe–O covalent structural bond environment of the Fe_3O_4 nanoparticles. However, the weak O–H and C–H peaks in Fig. 5 invariably point out that the amount of adsorbed surface polyol coating onto the nanoparticles is at its minimum. Therefore, in light of the above it must be understood in a manner that perhaps a lower reaction temperature from the present 300 °C may well lead to improve both the surface coating as well as the dispersability of the nanoparticles in aqueous solutions. Nevertheless, it can now be ensured that the polyol method is effective in synthesizing single phase cubic magnetite nanoparticles at temperatures of about 300 °C and the resultant nanoparticles with their surfaces being coated by a thin layer of biocompatible PEG ligands can further be suspendable in aqueous medium so as to make them suitable for biomedical applications.

3.4. Thermogravimetric analysis

Fig. 6a,b shows the TGA curves for both the samples of magnetite nanoparticles synthesized by two different iron precursor/PEG amount ratios (the first with 24 mM of $FeCl_2{\cdot}4H_2O$ in 80 ml of PEG without any soaking time before the reaction temperature, and the second with 12 mM of $FeCl_2{\cdot}4H_2O$ in 80 ml of PEG with 30 min soaking time at 200 °C). The TGA curves of both the samples are broadly characterized by three regions for weight loss in the temperature ranges of 25–160, 160–550 and 550–800 °C. The demarcation of the first region at 160 °C may be attributed to the crystallization, and the second demarcation at 550 °C and the weight loss thereafter for both the samples may be ascribed to the reduction of iron oxide after the loss of PEG coating. In the case of sample-I with less ratio of PEG to the precursor, the first weight loss corresponded to the evaporation of adsorbed water and ethanol, and the second weight loss is due to the decomposition of surface adsorbed PEG coating from the particles. The amount of weight loss in this case up to the second demarcation is about 2–3% only, as shown in Fig. 6a. In the case of sample-II with high ratio of PEG to the precursor, the first region of weight loss remains the same as with the case of sample-I due to the evaporation of adsorbed water and ethanol. But, in the second region there observed a higher rate of weight loss up to the refluxing temperature (330 °C) of the PEG, and beyond this temperature the weight loss has been gradual up to 550 °C. The total weight loss for this sample up to this second demarcation is about 3–4%, as is clearly evident from Fig. 6b. This higher rate of weight loss has been ascribed not only to the presence of larger amount of PEG on the particle surface but also to the corresponding higher loss of the same when the temperature moves fast the refluxing temperature. However, it can be inferred from the variation of this TGA curve that the larger amount of PEG coated on the surface of the nanoparticles could well lead to stabilize them in the solution, and also to inhibit their growth while resulting in smaller size of the particles for this sample.

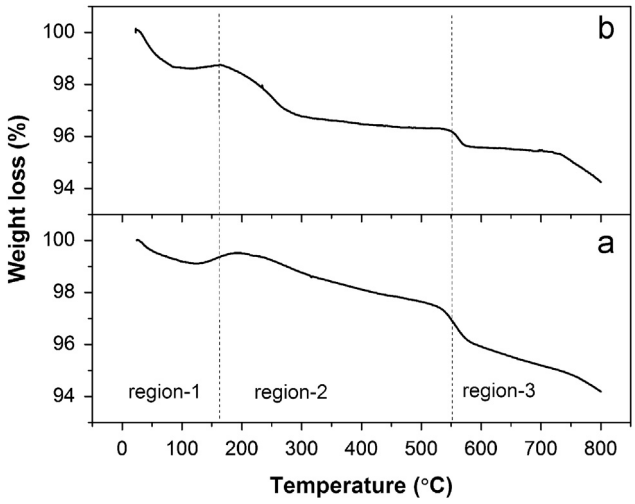

Fig. 6. TGA curves of the synthesized magnetite nanoparticles: (a) Sample-I, and (b) Sample-II.

3.5. Magnetic properties

The magnetic properties of the magnetite nanoparticles were measured at different temperatures of 5, 50, 100, 200 and 300 K using PPMS in an external magnetic field ranging from

−30 kOe to +30 kOe. Fig. 7a shows the magnetization curves for as-synthesized sample with particle sizes of about 32.3 nm. The saturation magnetization is 85.87 emu/g at 300 K with the coercivity of 120 Oe, and it increases with decreasing temperature to reach 91.7 emu/g at 5 K. This value of saturation magnetization, in fact, is quite close to the theoretical value of bulk magnetite (~92 emu/g) [19] and is perhaps, to our knowledge, the highest value ever of magnetization by polyol method for magnetite nanoparticles. This higher value may be attributed to the larger particle size with negligible surface spin disorder. It is well known from Neels' two sublattice model, the cation distribution of the magnetite nanoparticles of sample-I with mean particle size of 32.3 nm is completely inverse with the occupation of all the Fe^{2+} ions in octahedral sites while canceling the magnetic moments contributed by Fe^{3+} ions in tetrahedral and octahedral sites, thus facilitating the distribution to provide a strong A–B exchange interaction and contribute large enough magnetization. Moreover, the high crystallinity of the synthesized magnetite nanoparticles, as observed through the XRD patterns, also leads to a negligible surface spin canting and thus justifies the high value of magnetization [20].

Since the magnetization in nano scales is size dependent, the saturation magnetization value for the magnetite nanoparticles of sample-II with the mean particle size of about 9.2 nm is obtained to be 75 emu/g at 300 K (Fig. 7b). However, this decrease in magnetization value might not only be due to its reduced particle size but also due to the coating of a thin layer of PEG on the particles as indicated from FTIR and TGA curves leading to reduced mass. Also, another mechanism proposed here for low magnetization of this sample is due to the presence of spin canting at the particle surface [21], particularly in the particles for which the adsorbed surface coating is evaporated during the synthesis at the reaction temperature. In such case, the more the decrease in particle size, the larger the surface spin canting [22], and consequently a significant reduction in the magnetization value is obtained.

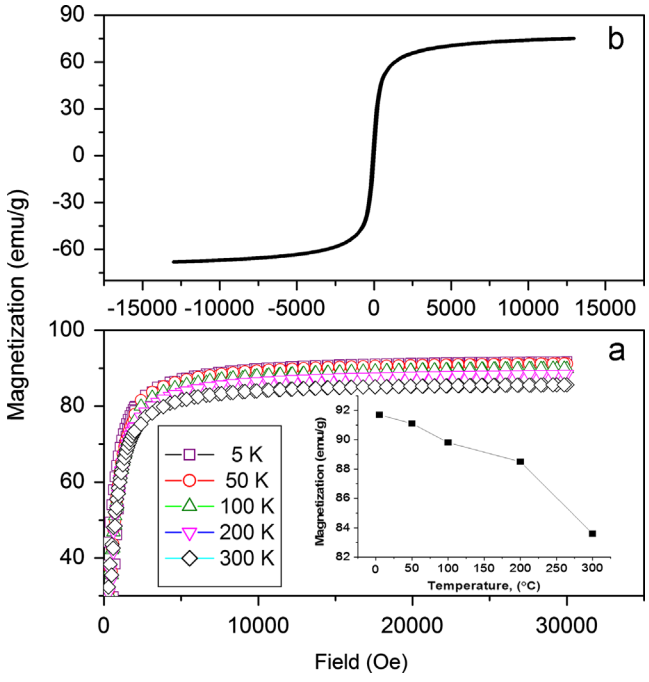

Fig. 7. (a) Magnetization curves of the magnetite nanoparticles of Sample-I measured at different temperatures of 5, 50, 100, 200 and 300 K using PPMS; inset of the figure shows the variation of magnetization with temperature, and (b) hysteresis loop of Sample-II.

4. Conclusions

In summary, we succeeded to synthesize high magnetization water soluble magnetite nanoparticles by a facile one-pot modified polyol method. Also, it has been successfully shown to control the size of the nanoparticles by modifying the reaction parameters such as iron precursor/PEG amount ratio, temperature and time of the reaction. The XRD studies confirm cubic spinel crystal structure while the TEM images indicate that the synthesized magnetite nanoparticles are almost spherical in shape. The saturation magnetization measured on the magnetite nanoparticles at 300 K is 85.87 emu/g and it increases with decreasing temperature to reach 91.7 emu/g at 5 K. However, the decrease in the mean particle size from about 32.3 nm to 9.2 nm resulted in a corresponding decrease in the magnetization to be 75 emu/g and this is attributed to the surface spin canting. The synthesized PEG coated magnetite nanoparticles are expected to be useful for biomedical applications due to their high saturation magnetization, increased biocompatibility and good hydrophilic properties. The ease and reproducibility of this simple polyol method ensures that we can easily fine tune the size, shape, surface adsorption and magnetic properties of the magnetite nanoparticles by further optimizing the reaction parameters.

Acknowledgments

This research was supported by WCU (World Class University) program through the National Research Foundation of Korea funded by the Ministry of Education, Science and Technology (R32-20026). Also we should thank Dr/ Hiroaki Kura from Tohoku University—Japan for helping us in measuring the magnetic properties of our sample.

References

[1] R. Weissleder, D.D. Stark, B.L. Engelstad, B.R. Bacon, C.C. Compton, D.L. White, P. Jacobes, J. Lewis, Superparamagnetic iron oxide: pharmacokinetics and toxicity, American Journal of Roentgenology 152 (1989) 167–173.

[2] Q.A. Pankhurst, J. Connolly, S.K. Jones, J. Dobson, Applications of magnetic nanoparticles in biomedicine, Journal of Physics D: Applied Physics 36 (2003) R167–R181.

[3] T. Neuberger, B. Schopf, H. Hofmann, M. Hofmann, B. von Rechenberg, Superparamagnetic nanoparticles for biomedical applications: possibilities and limitations of a new drug delivery system, Journal of Magnetism and Magnetic Materials 293 (2005) 483–496.

[4] Y. Xiong, J. Ye, X. Gu, Q.W. Chen, Synthesis and assembly of magnetite nanocubes into flux closure rings, Journal of Physical Chemistry C 111 (2007) 6998–7003.

[5] G.H. Gao, X.H. Liu, R.R. Shi, K.C. Zhou, Y.G. Shi, R.Z. Ma, Shape controlled synthesis and magnetic properties of monodisperse Fe_3O_4 nanocubes, Crystal Growth and Design 10 (2010) 2888–2894.

[6] M. George, A.M. John, S.S. Nair, P.A. Joy, M.R. Anantharaman, Finite size effects on the structural and magnetic properties of sol–gel synthesized $NiFe_2O_4$ powders, Journal of Magnetism and Magnetic Materials 302 (2006) 190–195.
[7] B. Parvatheeswara Rao, G.S.N. Rao, A. Mahesh Kumar, K.H. Rao, Y.L.N. Murthy, S.M. Hong, Chong-Oh Kim, CheolGi Kim, Soft chemical synthesis and characterization of$Ni_{0.65}Zn_{0.35}Fe_2O_4$ nanoparticles, Journal of Applied Physics 101 (123902) (2007) 1–4.
[8] F. Fievet, J.P. Lagier, M. Figlarz, Preparing monodisperse metal powders in micrometer and submicrometer sizes by the polyol process, MRS Bulletin 14 (1989) 29–34.
[9] G. Suresh, P. Saravanan, D. Rajan Babu, Synthesis of Fe–Co nanobars using sodium sulfite assisted polyol process and its structural, magnetic studies, Journal of Nano Research—SW (15) (2011) 21–28.
[10] Mohamed Abbas, Md. Nazrul Islam, B. Parvatheeswara Rao, Tomoyuki Ogawa, Migaku Takahashi, CheolGi Kim, One-pot synthesis of high magnetization air stable FeCo nanoparticles by modified polyol method, Materials Letters 91 (2013) 326–329.
[11] W. Cai, J. Wan, Facile synthesis of superparamagnetic magnetite nanoparticles in liquid polyols, Journal of Colloid and Interface Science 305 (2007) 366–370.
[12] D. Maity, P. Chandrasekharan, F. Si-Shen, Jun-Min Xue, J. Ding, Polyol-based synthesis of hydrophilic magnetite nanoparticles, Journal of Applied Physics 107 (2010) 09B310-1–09B310-3.
[13] R.H. Goncalves, C.A. Cardoso, E.R. Leite, Synthesis of colloidal magnetite nanocrystals using high molecular weight solvent, Journal of Materials Chemistry 20 (2010) 1167–1172.
[14] C. Cheng, F. Xu, H. Gu, Facile synthesis and morphology evolution of magnetic iron oxide nanoparticles in different polyol processes, New Journal of Chemistry 35 (2011) 1072–1079.
[15] A.A. Khaleel, Nanostructured pure γ-Fe_2O_3 via forced precipitation in an organic solvent, Chemistry—A European Journal 10 (2004) 925–932.
[16] Y.K. Sun, M. Ma, Y. Zhang, N. Gu, Synthesis of nanometer-size maghemite particles from magnetite, Colloids and Surfaces A: Physicochemical and Engineering Aspects 245 (2004) 15–19.
[17] B.D. Cullity, S.R. Stock, Elements of X-Ray Diffraction, 3rd ed., Prentice-Hall, Englewood Cliffs, NJ, 2001.
[18] J.R. Dyer, Applications of Absorption Spectroscopy of Organic Compounds, 6th ed., Prentice-Hall, Englewood Cliffs, NJ, 1965.
[19] D.H. Han, J.P. Wang, H.L. Luo, Crystallite size effect on saturation magnetization of fine ferrimagnetic particles, Journal of Magnetism and Magnetic Materials 136 (1994) 176–182.
[20] A.G. Roca, D. Niznansky, V.J. Poltierova, B. Bittova, G.M.A. Fernández, C.J. Serna, M.P. Morale, Magnetite nanoparticles with no surface spin canting, Journal of Applied Physics 105 (2009) 114309-1–114309-7.
[21] R.H. Kodama, A.E. Berkowitz, E.J. McNiff, S. Foner, Surface spin canting in $NiFe_2O_4$ nanoparticles, Physical Review Letters 77 (1996) 394–397.
[22] M. Rajendran, R.C. Pullar, A.K. Bhattacharya, D. Das, S.N. Chintalapudi, C.K. Majumdar, Magnetic properties of nanocrystalline $CoFe_2O_4$ powders prepared at room temperature: variation with crystallite size, Journal of Magnetism and Magnetic Materials 232 (2001) 71–83.